

PAPER

## Enhanced high-order harmonic generation driven by a wavefront corrected high-energy laser

To cite this article: Yang Wang *et al* 2018 *J. Phys. B: At. Mol. Opt. Phys.* **51** 134005

View the [article online](#) for updates and enhancements.

### Related content

- [The ELI-ALPS facility: the next generation of attosecond sources](#)  
Sergei Kühn, Mathieu Dumergue, Subhendu Kahaly *et al.*
- [Compact 200 kHz HHG source driven by a few-cycle OPCPA](#)  
Anne Harth, Chen Guo, Yu-Chen Cheng *et al.*
- [Collection and spectral control of high-order harmonics generated with a 50 W high-repetition rate Ytterbium femtosecond laser system](#)  
A Cabasse, Ch Hazera, L Quintard *et al.*





**IOP | ebooks™**

Bringing you innovative digital publishing with leading voices to create your essential collection of books in STEM research.

Start exploring the collection - download the first chapter of every title for free.

# Enhanced high-order harmonic generation driven by a wavefront corrected high-energy laser

Yang Wang<sup>1</sup>, Tianyi Guo<sup>1</sup>, Jialin Li<sup>1</sup>, Jian Zhao<sup>1</sup>, Yanchun Yin<sup>1</sup> , Xiaoming Ren<sup>1</sup>, Jie Li<sup>1</sup>, Yi Wu<sup>1</sup>, Matthew Weidman<sup>1,2</sup>, Zenghu Chang<sup>1</sup>, Marieke F Jager<sup>3</sup>, Christopher J Kaplan<sup>3</sup>, Romain Geneaux<sup>3</sup> , Christian Ott<sup>3</sup>, Daniel M Neumark<sup>3</sup> and Stephen R Leone<sup>3,4</sup>

<sup>1</sup>Institute for the Frontier of Attosecond Science and Technology, CREOL and Department of Physics, University of Central Florida, Orlando, FL 32816, United States of America

<sup>2</sup>Max Planck Institute of Quantum Optics, PO Box 13 27, D-85741 Garching, Germany

<sup>3</sup>Department of Chemistry and Physics, University of California, Berkeley, CA 94720, United States of America

<sup>4</sup>Chemical Sciences Division, Lawrence Berkeley National Laboratory, Berkeley, CA 94720, United States of America

E-mail: [Zenghu.Chang@ucf.edu](mailto:Zenghu.Chang@ucf.edu)

Received 31 December 2017, revised 18 April 2018

Accepted for publication 17 May 2018

Published 11 June 2018



CrossMark

## Abstract

We developed and implemented an experimental setup for the generation of high-energy high-order harmonics in argon gas for nonlinear experiments in the extreme ultraviolet (XUV) spectral range. High-order harmonics were generated by loosely focusing a high-energy laser pulse centered around 800 nm into a gas cell filled with argon in a phase-matching condition. The wavefront distortions of the driving pulse were corrected by a deformable mirror, and the XUV conversion efficiency was significantly improved due to the excellent beam profile at focus. A high-damage-threshold beam splitter was used to eliminate high-energy driving pulses co-propagating with high-order harmonics. The setup has a potential to provide intense ultrashort XUV pulses reaching the intensity levels required for nonlinear experiments in the XUV spectral range.

Keywords: high-order harmonics, XUV, wavefront, high flux attosecond

## Introduction

High-order harmonics generated (HHG) by the interaction of an ultrafast high power laser with atoms and molecules is recognized as a very attractive coherent short-wavelength light source [1]. HHG has been applied to many research areas such as attosecond science, plasma physics, high-resolution imaging, spectroscopy and nonlinear optics in the extreme ultraviolet (XUV) region [2]. At the single atom level, HHG can be explained by the semiclassical three-step/recollision model [3] and its quantum counterpart based on the strong field approximation [4]. The experimentally observed high harmonic signals are strongly affected by macroscopic phase-matching processes. At the present time,

theories and simulations are still not able to quantitatively predict the high harmonic yields for a given experimental condition. It is important to collect experimental data under different conditions to help the development of quantitative recollision theories.

Currently, the energy of XUV pulses available is limited by the low conversion efficiency and the energy of the driving laser. For the further development of a variety of applications, one of the most important issues is XUV pulse energy scaling [5]. Rudawski *et al* have generated 200 nJ per pulse and per harmonic order in argon [6]. A number of groups [7–9] have generated  $\mu$ J-level harmonic energy in the XUV region in pulse trains. The increase of harmonic energy is linearly dependent on the focusing area of the driving pulse. This

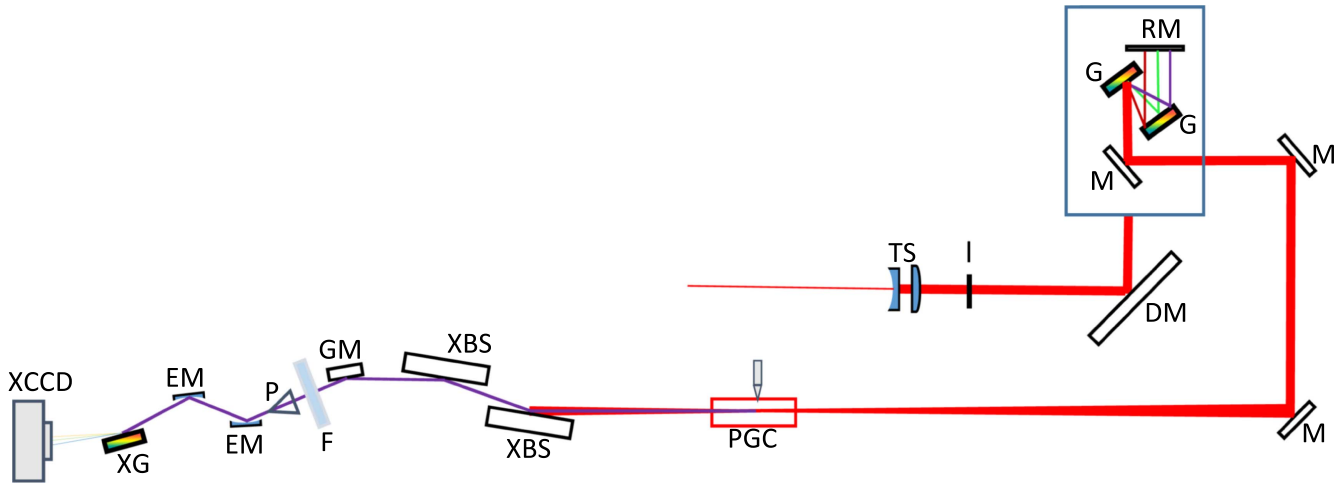


**Figure 1.** Experimental setup with a  $f = 25$  m focusing configuration: TS—telescope, I—iris, DM—deformable mirror, M—folding mirror, G—grating, RM—roof mirror, PGC—pulsed gas cell, XBS—XUV beam splitter, GM—gold mirror, F—aluminum filter, P—XUV photodiode, EM—ellipsoidal mirror, XG—XUV grating, XCCD—XUV CCD camera.

energy scaling method can be universally applied to HHG in neutral gases. A loosely focused beam with an excellent beam quality is required for the phase-matching condition in a long interaction length.

Unfortunately, in chirped pulse amplification (CPA) laser systems with joule level pulse energies, geometrical aberrations and surface quality from optical components, thermal effects and inhomogeneous doping in Ti:Sapphire crystals affect the beam profile and focusability, degrading the energy distribution and wavefront (WF) [10]. A large portion of the pulse energy will be spread out into the wings of the focal spot.

Another challenge is the separation of the high-intensity pump pulse from the co-propagating harmonics. It is necessary to attenuate the intensity of the pump pulses to less than one hundred gigawatts per square centimeter to avoid damaging the XUV optics or samples placed in the beam. Nagata *et al* reported a beam splitter (BS) for wavelengths shorter than 30 nm, which used a 10 nm thick niobium nitrogen ( $N_bN$ ) film prepared on a Si substrate [11]. However, the low damage-threshold of Si restricted the pump laser to the level of hundreds of millijoules  $cm^{-2}$ .

In this study, we present progress towards finding the solutions to these two challenges.

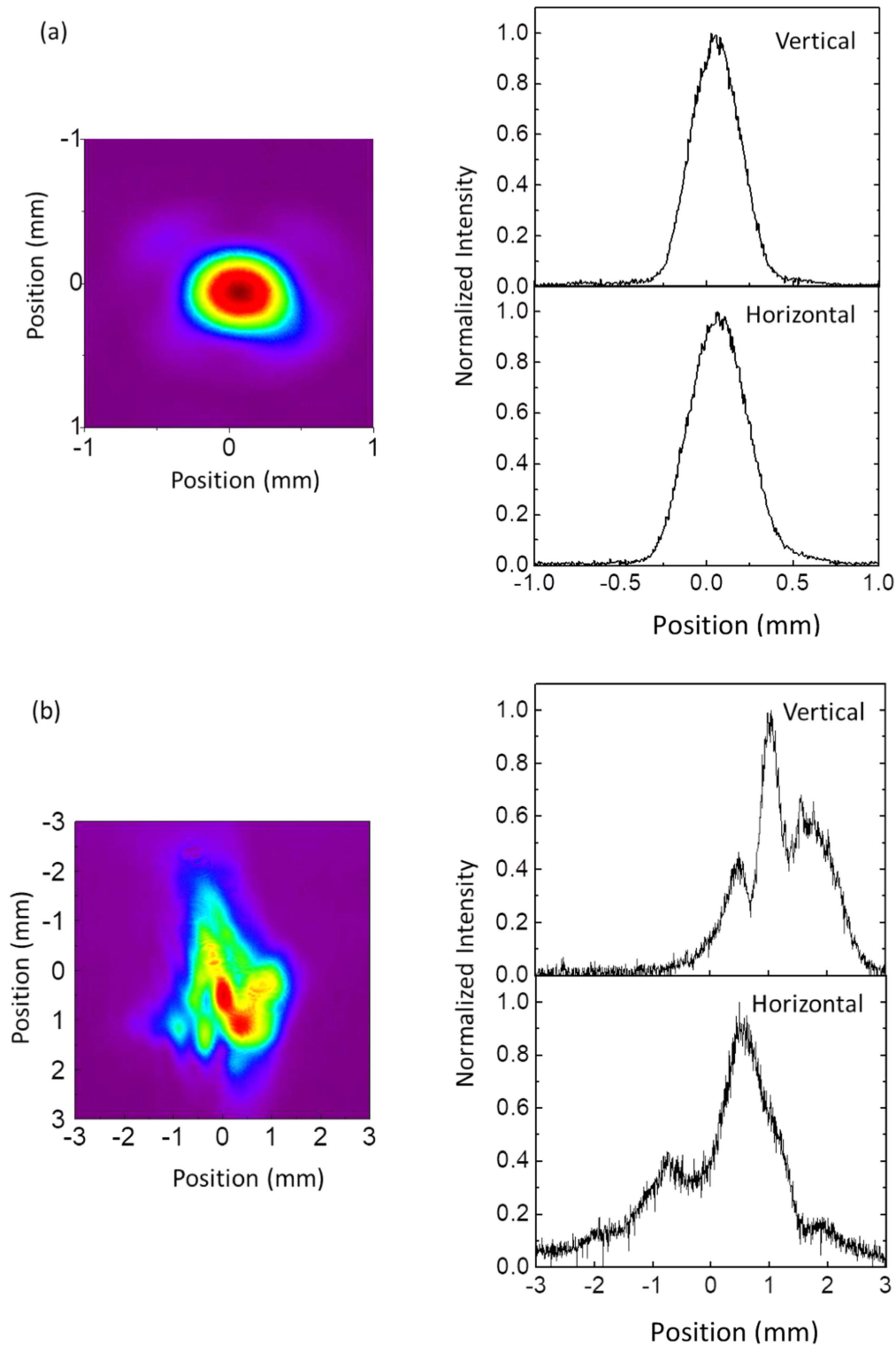
## Experimental setup, results and discussions

Figure 1 illustrates the HHG generation setup, which consists of four sections: the laser system [12], HHG generation, experimental pump-probe station, and diagnostics. The sections are connected by vacuum tubes and chambers.

The experimental studies were carried out using a three-stage 10 Hz Ti:Sapphire CPA laser system pumped by flash-lamp-pumped Nd:YAG lasers. The system produces an output of 1 J pulse energy with a center wavelength at 800 nm, a pulse duration of 35 fs, and a beam diameter of 68 mm.

The deformable mirror (DM) has been applied to a low-energy Ti:Sapphire laser to optimize high-order harmonics [13–16]. In this paper, we used a DM to correct the wavefront of a Ti:Sapphire laser at the joule energy level to improve the beam profile at the focal point and thus increase the effective interaction intensity. In addition, we designed a high-reflectivity, high-damage-threshold BS for wavelengths shorter than 50 nm. The absolute energy of HHG was measured directly with an unbiased silicon XUV photodiode, and the XUV spectrum was recorded by a calibrated XUV charge-coupled device (CCD) camera.

The driving pulse was loosely focused by a telescope, which includes one plano-concave lens and one plano-convex lens with a focal length of  $-600$  mm and  $1600$  mm, respectively. By varying the separation of the two lenses, a tunable focal length can be achieved. This is of great importance for the control of the beam size, which allows for re-adjustment of the focusing geometry as well as the intensity distribution at the focus and thus allows us to optimize the phase-matching condition and increase the XUV pulse energy in a simple way. An  $f = 25$  m loose focusing geometry in the HHG generation cell was employed in our HHG setup. The pump beam size was increased to 68 mm before the compressor by a telescope to avoid damaging the optical components. The WF of the pump pulse was corrected by a DM [17]. The WF distribution of the pump pulse was measured with a Shack–Hartman sensor. The measurement results are used to feedback control the DM to correct the driving laser WF distortions. The root mean square (rms) of the WF distribution was reduced from 600 to 25 nm, corresponding to a value of  $\lambda/32$ , where  $\lambda$  is the center wavelength of the driving pulse. The effects of the WF distortions on the beam profile at focus are shown in figure 2. Nearly a diffraction-limited beam with a diameter of  $650 \mu m$  (full width at half maximum of the intensity) was obtained after the correction, which increased the effective intensity at the focal point by one order of magnitude.



**Figure 2.** Driving pulse beam profile at focus with (a) and without (b) wavefront correction.

In the generation chamber, the interaction gas cell has a diameter of 4.6 mm and a length of 100 mm. There are two small holes at the entry and exit of the cell for differential pumping. The diameter of the holes is about 0.8 mm. The gas was released at a repetition rate of 10 Hz controlled by a valve driven by a piezo-electric actuator and synchronized with the laser pulse. The valve can provide sufficient gas inside the gas

cell allowing good phase-matching. To maximize the HHG signal, we optimized the opening time of the valve. The HHG beam and the driving laser beam propagate collinearly to the XUV BS chamber.

A designed XUV BS was used to transmit the fundamental laser and reflect XUV. Tantalum pentoxide ( $\text{Ta}_2\text{O}_5$ ) is a high-quality thin film material that can be deposited on a

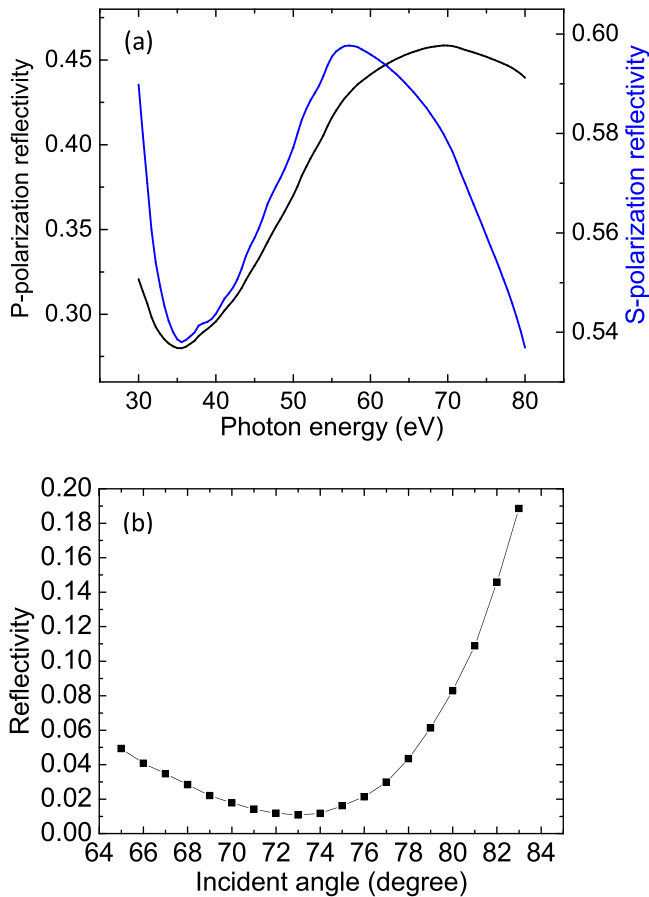


**Figure 3.** (a) Calculated reflectivity for XUV BS as a function of the XUV photon energy for both s- (blue) and p-polarization (black) at an incident angle of  $73^\circ$ , (b) measured IR reflectivity of XUV BS as a function of the incident angles for the p-polarized driving pulses.

fused silica ( $\text{SiO}_2$ ) substrate by sputtering. The BS was coated with five layers of  $\text{SiO}_2/\text{Ta}_2\text{O}_5$  films, which has a low attenuation ratio and a high-damage-threshold intensity of at least  $100 \text{ TW cm}^{-2}$  for the 35 fs driving pulses. The reflectivity for the XUV light was calculated from the complex refractive indices of the  $\text{Ta}_2\text{O}_5$  film and fused silica [18]. Figure 3(a) shows the calculated reflectivity of  $\text{Ta}_2\text{O}_5$  film deposited on  $\text{SiO}_2$  substrates as a function of the wavelength for both s- and p-polarized HHG. The experimental results show that the actual reflectivity is smaller than the calculated one because of the roughness on the coating surface [18]. Reflectivity of the 35 fs, 800 nm, p-polarized pump pulses was measured as a function of incident angle presented in figure 3(b). The minimum reflectivity was 1%, which was achieved at an incident angle of  $73^\circ$  for the p-polarization, while it is  $\sim 78\%$  for the s polarization. The two BSs were placed orthogonally to attenuate both s- and p-polarized driving laser to facilitate the gating technique for the isolated attosecond pulses in the near future [19]. Afterwards, a 200 nm thick aluminum (Al) filter is used to completely remove the fundamental beam.

The absolute energy of the HHG was measured directly with a silicon XUV photodiode (AXUV 100), which covers a wide spectral range. The quantum efficiency and sensitivity

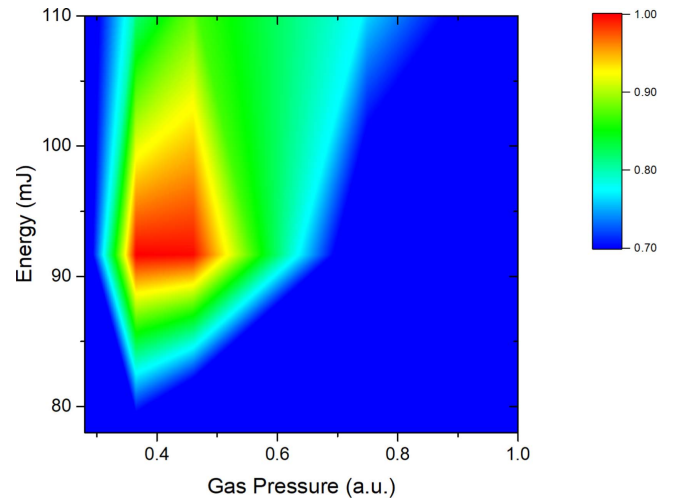


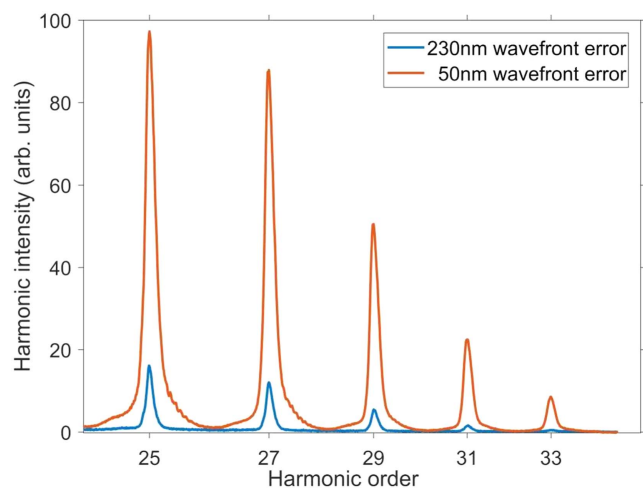
**Figure 4.** Intensity of the total harmonics generated in argon as a function of the generation gas pressure and driving laser energy.

are given in [20]. The signal from the detector was recorded by an oscilloscope. The measured XUV pulse energy corresponds to an estimated pulse energy of  $0.3 \mu\text{J}$  at the exit of the gas cell, assuming a total 1% throughput for the two XUV separators, a gold mirror and a 200 nm Al filter with oxidation layers [21].

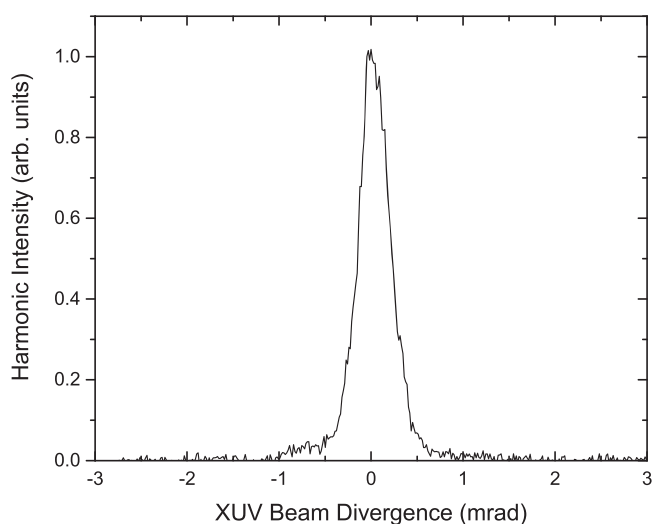
Two ellipsoidal mirrors coated with gold were placed in the experimental chamber to tightly focus the XUV beam to a diameter of  $8 \mu\text{m}$ . The ellipsoidal mirrors imaged the XUV beam into an XUV spectrometer located in the diagnostics chamber. A grazing incidence, aberration corrected concave grating (Hitachi 001-0640 XUV) was used to disperse the XUV spectra to an XUV CCD camera. The following parameters were carefully controlled in order to achieve the best phase-matching condition: fundamental pulse energy, gas pressure, gas cell position relative to the laser focus, focus beam profile and size. The dependence of the total harmonics generated in argon as a function of the gas pressure and pump pulse energy after the WF correction is shown in figure 4. We recorded a set of HHG spectra while varying the gas pressure. The signal is normalized to the maximum obtained for total harmonics. The gas pressure in the cell is adjusted by controlling the backing pressure applied to the nozzle.

Figure 5 shows the typical harmonic spectra for two different driving laser WF distortions in argon under the phase-matching condition. The rms of the WF distortion was measured to be 50 nm and 230 nm, respectively, with and without the DM. The phase-matching condition was optimized for the total energy yield of HHG. Low-orders ( $< 21\text{st}$ ) are strongly absorbed in argon gas [5]. The input laser energy and medium length were 90 mJ and 100 mm, respectively. With a better WF correction, the harmonic signal was enhanced by more than nine times and the conversion efficiency was improved by a factor of 18. With a larger  $f$  number ( $f = 75 \text{ m}$ ), the full pulse energy (1 J) can be applied to boost the XUV pulse energy by more than one order of magnitude.

Figure 6 depicts the far-field spatial profile of the 25th harmonic. The profiles were integrated with respect to



**Figure 5.** Experimental harmonic spectra in Ar gas driven by pump lasers with 50 nm wavefront error corrected by a DM and with 230 nm wavefront error without wavefront correction.



**Figure 6.** Normalized 1D distribution of the 25nd harmonic in Ar gas.

wavelength. The output beam divergence was estimated to be  $\sim 0.4$  mrad (FWHM) compared with the driving laser divergence of  $\sim 1.5$  mrad.

## Conclusions

In summary, we have developed a high-energy HHG setup and generated a total energy of  $0.3 \mu\text{J}$  HHG per laser pulse in argon by a loosely focusing geometry. The beam quality of the focused high-energy laser pulse was significantly improved by correcting WF distortions using a DM, resulting in an improvement of the XUV conversion efficiency. We produced an XUV BS with a high-damage-threshold of  $100 \text{ TW cm}^{-2}$ . The XUV source is designed for future studies of nonlinear processes in the XUV spectral range and the attosecond pump-probe experiment. The estimated XUV intensity at focus is  $\sim 10^{14} \text{ W cm}^{-2}$ , which is sufficient to

induce nonlinear optical phenomena in the XUV region such as the multiphoton ionization processes and the above-threshold ionization of He or two-photon double ionization of neon [22–24]. The conversion efficiency can be held constant when changing the focal length, if the gas pressure, the laser pulse energy, and the medium length are scaled appropriately. By applying this scaling procedure, the harmonic pulse with energy as high as tens of  $\mu\text{J}$  could be reached using a loose focusing geometry of  $f = 100 \text{ m}$  with a joule level pump laser. The true attosecond pump attosecond-probe experiments can be conducted with such a high attosecond pulse energy [25, 26].

## Acknowledgments

This work has been supported by the DARPA PULSE program with grants from AMRDEC (W31P4Q1310017), Army Research Office (W911NF-14-1-0383), Air Force Office of Scientific Research (FA9550-15-1-0037, FA9550-16-1-0013), and National Science Foundation (1506345).

## ORCID iDs

Yanchun Yin  <https://orcid.org/0000-0001-9034-1738>

Romain Geneaux  <https://orcid.org/0000-0002-3395-6813>

## References

- [1] Chang Z and Corkum P B 2010 Attosecond photon sources: the first decade and beyond *J. Opt. Soc. Am. B* **27** B9
- [2] Sansone G, Poletto L and Nisoli M 2011 High-energy attosecond light sources *Nat. Photon.* **5** 655
- [3] Corkum P B 1993 Plasma perspective on strong field multiphoton ionization *Phys. Rev. Lett.* **71** 1994
- [4] Lewenstein M, Balcou P, Ivanov M Y, L’Huillier A and Corkum P B 1994 Theory of high-harmonic generation by low-frequency laser fields *Phys. Rev. A* **49** 2117
- [5] Takahashi E, Nabekawa Y, Otsuka T, Obara M and Midorikawa K 2002 Generation of highly coherent submicrojoule soft x rays by high-order harmonics *Phys. Rev. A* **66** 021802
- [6] Rudawski P *et al* 2013 A high-flux high-order harmonic source *Rev. Sci. Instrum.* **84** 073103
- [7] Hergott J-F, Kovacev M, Merdji H, Hubert C, Mairesse Y, Jean E, Breger P, Agostini P, Carré B and Salières P 2002 Extreme-ultraviolet high-order harmonic pulses in the microjoule range *Phys. Rev. A* **66** 021801
- [8] Takahashi E, Nabekawa Y and Midorikawa K 2002 Generation of  $10 \mu\text{J}$  coherent extreme-ultraviolet light by use of high-order harmonics *Opt. Lett.* **27** 1920
- [9] Yoshitomi D, Shimizu T, Sekikawa T and Watanabe S 2002 Generation and focusing of submilliwatt-average-power 50 nm pulses by the fifth harmonic of a KrF laser *Opt. Lett.* **27** 2170
- [10] Ranc S, Chériaux G, Ferré S, Rousseau J-P and Chambaret J-P 2000 Importance of spatial quality of intense femtosecond pulses *Appl. Phys. B* **70** S181

- [11] Nagata Y, Nabekawa Y and Midorikawa K 2006 Development of high-throughput, high-damage-threshold beam separator for 13 nm high-order harmonics *Opt. Lett.* **31** 1316
- [12] Wu Y, Cunningham E, Li J, Zang H, Chini M, Wang X, Wang Y, Zhao K and Chang Z 2013 Generation of high-flux attosecond extreme ultraviolet continuum with a 10 Terawatt laser *Appl. Phys. Lett.* **102** 201105
- [13] Villorosi P, Bonora S, Pascolini M, Poletto L, Tondello G, Vozzi C, Nisoli M, Sansone G, Stagira S and Silvestri S D 2004 Optimization of high-order harmonic generation by adaptive control of a sub-10-fs pulse wave front *Opt. Lett.* **29** 207
- [14] Winterfeldt C, Spielmann C and Gerber G 2008 Colloquium: optimal control of high-harmonic generation *Rev. Mod. Phys.* **80** 117
- [15] Bandulet H-C, Comtois D, Shiner A D, Trallero-Herrero C, Kajumba N, Ozaki T, Corkum P B, Villeneuve D M, Kieffer J C and Légaré F 2008 High harmonic generation with a spatially filtered optical parametric amplifier *J. Phys. B: At. Mol. Opt. Phys.* **41** 245602
- [16] Heyl C M, Arnold C L, Couairon A and L'Huillier A 2017 Introduction to macroscopic power scaling principles for high-order harmonic generation *J. Phys. B: At. Mol. Opt. Phys.* **50** 013001
- [17] Druon F, Chériaux G, Faure J, Nees J, Nantel M, Maksimchuk A, Mourou G, Chanteloup J C and Vdovin G 1998 Wave-front correction of femtosecond terawatt lasers by deformable mirrors *Opt. Lett.* **23** 1043
- [18] Henke B L, Gullikson E M and Davis J C 1992 X-ray interactions: photoabsorption, scattering, transmission, and reflection at  $E = 50\text{--}30\,000$  eV,  $Z = 1\text{--}92$  *At. Data Nucl. Data Tables* **54** 181
- [19] Feng X, Gilbertson S, Mashiko H, Wang H, Khan S D, Chini M, Wu Y, Zhao K and Chang Z 2009 Generation of isolated attosecond pulses with 20 to 28 femtosecond LASERS *Phys. Rev. Lett.* **103** 183901
- [20] Krumrey M, Tegeler E, Goebel R and Köhler R 1995 Self-calibration of the same silicon photodiode in the visible and soft x-ray ranges *Rev. Sci. Instrum.* **66** 4736
- [21] Powell F R, Lindblom J F, Powell S F and Vedder P W 1990 Thin film filter performance for extreme ultraviolet and x-ray applications *Opt. Eng., Bellingham* **29** 614
- [22] Hasegawa H, Takahashi E J, Nabekawa Y, Ishikawa K L and Midorikawa K 2005 Multiphoton ionization of He by using intense high-order harmonics in the soft-x-ray region *Phys. Rev. A* **71** 023407
- [23] Manschwetus B et al 2016 Multiphoton ionization of He by using intense high-order harmonics in the soft-x-ray region *Phys. Rev. A* **93** 061402
- [24] Takahashi E J, Lan P F, Mu'cke O D, Nabekawa Y and Midorikawa K 2013 Attosecond nonlinear optics using gigawatt-scale isolated attosecond pulses *Nat. Commun.* **4** 2691
- [25] Hu S and Collins L 2006 Attosecond pump probe: exploring ultrafast electron motion inside an atom *Phys. Rev. Lett.* **96** 073004
- [26] Campi F, Coudert-Alteirac H, Miranda M, Rading L, Manschwetus B, Rudawski P, L'Huillier A and Johnsson P 2016 Design and test of a broadband split-and-delay unit for attosecond XUV–XUV pumpprobe experiments *Rev. Sci. Instrum.* **87** 023106